

Dye-sensitized solar cells fabricated with size-selected titanium dioxide nanowires via an electrospinning method

Suk In Noh and Hyo-Jin Ahn*

Department of Materials Science & Engineering, Seoul National University of Science and Technology, Seoul, 139-743, Korea

Two types of size-selected titanium dioxide (TiO₂) nanowires (NWs) have been successfully synthesized via an electrospinning method and their structural and photovoltaic features investigated for use as a photoelectrode in dye-sensitized solar cells (DSSCs). Scanning electron microscopy (SEM), transmission electron microscopy (TEM), X-ray diffraction (XRD), and X-ray photoelectron spectroscopy (XPS) results show that two types of size-selected TiO₂ NWs, which are made of anatase and rutile phases, have average diameters of ~100 nm and ~30 nm. Photocurrent-voltage curves show that the TiO₂ NW photoelectrodes fabricated with a ~30 nm diameter exhibit a superior short-circuit current density of 10.86 mA/cm² and a cell efficiency of 3.93%, for an area of 0.196 cm² compared to those fabricated with a ~100 nm diameter, which is attributed to the increased specific surface area that allows for a higher rate of dye adsorption.

Key words: Electrospinning, TiO₂, Nanowires, Photovoltaic studies, Dye-sensitized solar cells.

Introduction

Dye-sensitized solar cells (DSSCs) are composed of a nano-sized TiO₂ photoelectrode sensitized by dye molecules, an electrolyte, a counter electrode, and a transparent conducting substrate. They have been of great interest because of the advantages such as low-cost fabrication, a less toxic manufacturing environment, and flexibility of devices compared with the conventional solid state junction devices [1, 2]. Several factors may affect the performance in DSSCs, such as the size and structure of the electrodes, the size of the electrode's holes, the chemical properties of the dye, the electrical properties of the electrolyte, electrical and structural properties of the counter electrode, the ability to absorb light, the intensity of the light, and et al. [3]. Of these factors, the size and the structure of the electrodes are important for improving photovoltaic efficiency in DSSCs. Indeed, TiO₂ nanoparticles have been most widely used as anode materials for DSSCs [4, 5], and now, TiO₂ is currently one of most interesting materials used as a photoanode in DSSCs because of the low-cost, easy controllability of its morphology, and its chemical stability [6].

One-dimensional nanostructured photoelectrodes in DSSCs have recently been studied extensively in regards to the morphology of materials because of their unique electrical, electrochemical, and optical properties [6-8]. For example, Mukherjee et al. reported that electrospun TiO₂ nanofibers with a diameter of ~150 nm in

DSSCs exhibit effective electron diffusion coefficients due to their polycrystalline nature and random web structure [9]. Onozuka et al. reported DSSCs comprising of TiO₂ nanofibers with high surface areas via electrospinning. TiO₂ nanofibers fabricated with a diameter of ~250 nm showed a cell efficiency of 4.4% in an adjusted membrane thickness of 3.9 μm [10]. More recently, Oh et al. studied the fabrication of TiO₂ branched nanowires using a seeding method for DSSCs and obtained an improved short-circuit current density and cell efficiency of 12.18 mA/cm² and 4.3% compared to the TiO₂ nanowires [11]. In particular, in the case of one-dimensional nanostructures, the efficiency of the DSSCs was mainly limited by low dye adsorption and low surface area of one-dimensional NWs [12]. Therefore, a study between the photovoltaic properties and the size/structure of electrodes in one-dimensional nanostructures for use as a photoelectrode in DSSCs still remains.

In this work, two types of size-selected TiO₂ NWs were synthesized via electrospinning and a relationship between their size/structure and photovoltaic properties was demonstrated. Also, an electrospinning method was used to fabricate TiO₂ NWs for use as a photoanode in DSSCs because of the several advantages, such as a simple process, easy controllability of NW dimensions, and good repeatability [13-16].

Experimental Procedures

A titanium precursor solution consisting of Ti (OiPr)₄ (Aldrich) and acetic acid (Aldrich) was mixed with 3 ml of anhydrous ethanol (Aldrich) and constantly stirred for approximately ten minutes. Then it was added into 7.5 ml of ethanol that contained 0.45 g of

*Corresponding author:
Tel : +82-2-970-6622
Fax: +82-2-973-6657
E-mail: hjahn@seoultech.ac.kr

Polyvinylpyrrolidone (PVP, $M_w = 1,300,000$ g/mol). The mixed solution for electrospinning was left to rest for thirty minutes before it was loaded into the syringe pump.

Among the several parameters in an electrospinning technique, an applied voltage and a needle gauge are important in controlling the size of the NWs. For TiO_2 NWs having a diameter of ~ 100 nm, a 23-gauge stainless steel needle was equipped on a 12 ml plastic syringe. The feeding rate was controlled to 0.04 ml/h under an applied voltage of ~ 8 kV. For TiO_2 NWs having a diameter of ~ 30 nm, a 32-gauge needle was used, and the feeding rate was controlled to 0.10 ml/h under an applied voltage of ~ 20 kV. The distance of the needle and collector was fixed to ~ 8 cm in both cases. Aluminum foil was used as a collector as well. Calcination at 500°C for five hours was carried out to selectively eliminate polymer. The morphologies of the samples were measured by field emission scanning electron microscopy (FE-SEM, Hitachi S-4100) and transmission electron microscopy (TEM, TECNAI-F20). The crystallinity and chemical bonding states of the samples were carried out by X-ray diffraction (XRD, Rigaku Rint 2500 with a $\text{Cu K}\alpha$ radiation) and X-ray photoemission spectroscopy (XPS, ESCALAB 250 with an $\text{Al K}\alpha$ X-ray source). For the light absorption properties of the samples, a UV-Visible spectrophotometer (UV-Vis), the Jasco V650, was used and it measured in the range of 200 nm to 900 nm.

DSSCs were fabricated by a conventional method to investigate photovoltaic efficiency of the size-selected TiO_2 NWs. Ground paste, the weight of which consisted of 16.2% of TiO_2 , 11.9% of hydroxypropyl cellulose (HPC, $M_w \sim 80,000$, Aldrich), 4.4% of acetyl acetone, and 67.5% of DI (De-ionized) water, was applied on an F-doped SnO_2 (FTO, $15 \Omega/\text{cm}^2$) coated glass using a squeeze printing in the size of 0.196 cm^2 , and afterwards annealed at 500°C for one hour and then immersed into the 0.5 mM/L of Ru-535-bisTBA, known as N719, (Solaronix) solution as well. A platinum covered counter electrode and an as-prepared working electrode were overlapped and an electrolyte was filled between the counter and working electrode. Photocurrent-voltage curves were measured under the irradiation of a 150 watt xenon lamp (LAB 50) together with the level of standard irradiance (AM 1.5 simulated sunlight) with an intensity of $100 \text{ mW}/\text{cm}^2$.

Results and Discussion

Figure 1 shows SEM images of size-selected TiO_2 NWs having two different diameters after calcination at 500°C . All the samples represent the morphology of uniform NWs. Two types of the size-selected TiO_2 NWs have average diameters of ~ 100 nm and ~ 30 nm, respectively. Figure 2 presents TEM images of the NWs obtained from an electrospinning method. The TiO_2 NWs of Figure 2(a) and Figure 2(b) are shown to

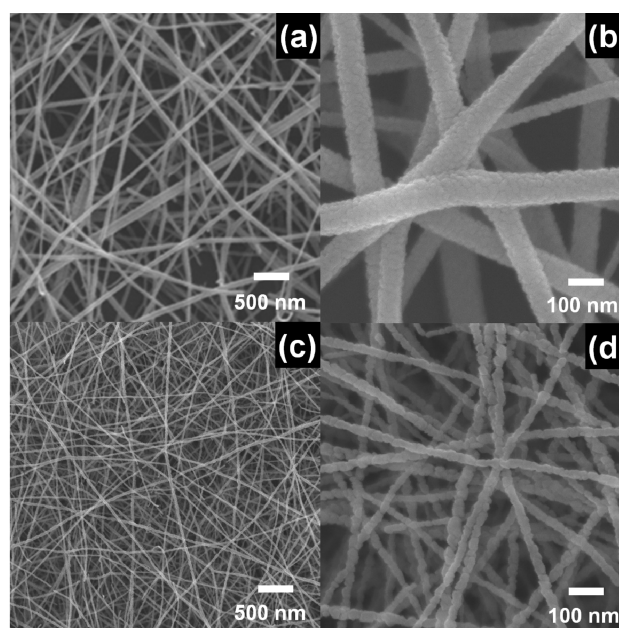


Fig. 1. SEM images of TiO_2 NW photoelectrodes with (a) ~ 100 nm and (c) ~ 30 nm in diameter after calcination at 500°C . Figure (b) and (d) present enlarged SEM images of Figure (a) and (c), respectively.

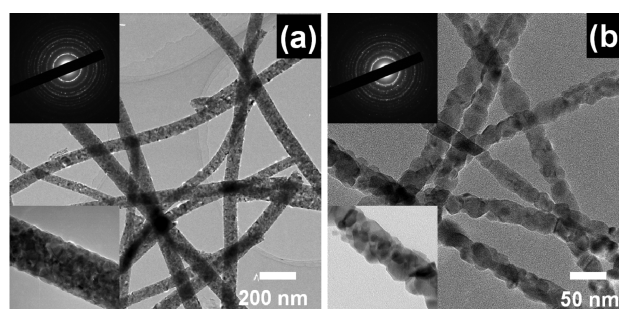


Fig. 2. The TEM images of the TiO_2 NW photoelectrodes with (a) ~ 100 nm and (b) ~ 30 nm in diameter fabricated via electrospinning. The insets exhibit SAED patterns and enlarged TEM images of the samples.

be ~ 100 nm and ~ 30 nm in diameter, respectively. TiO_2 NWs with ~ 100 nm diameter and with ~ 30 nm diameter seem to be composed of nanoparticles (or nano-grains) with 5–10 nm size and 10–20 nm size as shown in the insets of Figure 2. Two types of TiO_2 NWs having ~ 100 nm diameter and ~ 30 nm diameter reveal diffuse ring-like patterns containing spots around (000) plane, indicating that their polycrystalline properties are well in agreement with the XRD results.

To further investigate the structure and crystallinity of all the NWs, XRD examinations were carried out as shown in Figure 3. Crystal structures of electro-spun TiO_2 NWs consist of anatase and rutile phases. That is, the XRD peaks of two samples are in good agreement with those of anatase TiO_2 structure (25.3° , 37.8° , 48.0° , 53.8° , 62.7° , and 68.8° , space group $I4_1/amd$ (141)) [JCPDS card No. 841286] and rutile TiO_2 structure (27.4° , 36.0° , 41.2° , 54.3° , and 56.6° , space group $p4_2/$

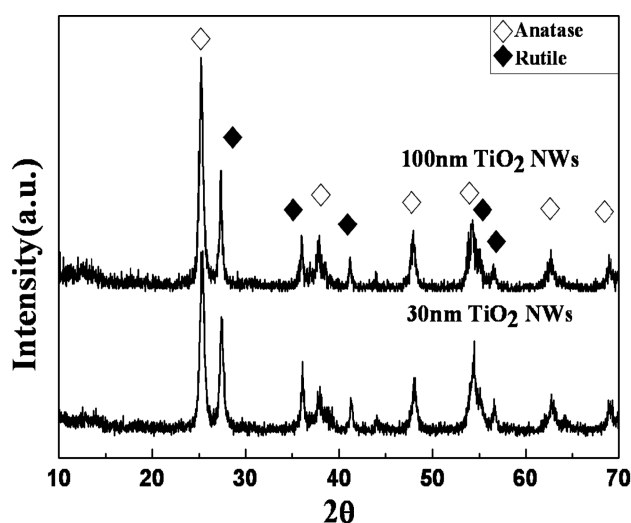


Fig. 3. Powder XRD patterns of the TiO₂ NW photoelectrodes with (a) ~100 nm and (b) ~30 nm in diameter, measured in the range of 10° to 70°.

mm (136)) [JCPDS card No. 870920]. Furthermore, the peak intensity of the (101) plane at 25.2° on the anatase phases is higher than that of the (110) plane at 27.4° on the rutile phases as shown in Figure 3. This implies that all the samples of the electro-spun TiO₂ NWs are mainly formed along the (101) of the anatase phases rather than the (110) of the rutile phases.

Figure 4 represents the XPS spectra obtained from two samples to examine the chemical bonding states of titanium and oxygen atoms. Figure 4(a) and 4(b) exhibit the XPS core-level spectra for the Ti 2p_{3/2} and Ti 2p_{1/2} photoelectrons at ~458.4 eV and ~464.0 eV for

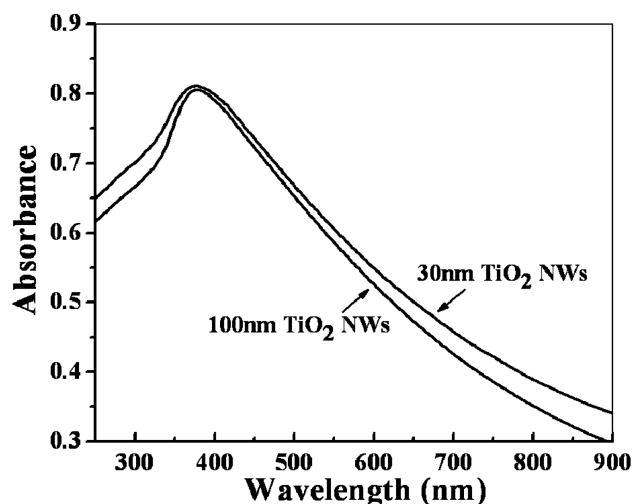


Fig. 5. UV-Vis absorption spectra obtained from the size-selected TiO₂ NWs with ~30 nm and ~100 nm in diameter.

two types of TiO₂ NWs having a ~100 nm diameter and a ~30 nm diameter, respectively. This implies that the elemental titanium in the TiO₂ is existing not as a Ti(II) species, but a Ti(IV) species. Figure 4(c) and 4(d) exhibit the XPS core-level spectra for the oxygen 1s photoelectrons at ~529.6 eV for two samples with a ~100 nm diameter and a ~30 nm diameter, indicating that the elemental oxygen species in the TiO₂ is existing as an O(II) species, which arises from the bulk oxygen atoms [17]. The second set of oxygen 1s is observed at ~530.9 eV corresponding to the bridging oxygen groups [18]. Although two kinds of oxygen atoms exist at the surface on the TiO₂ NWs fabricated

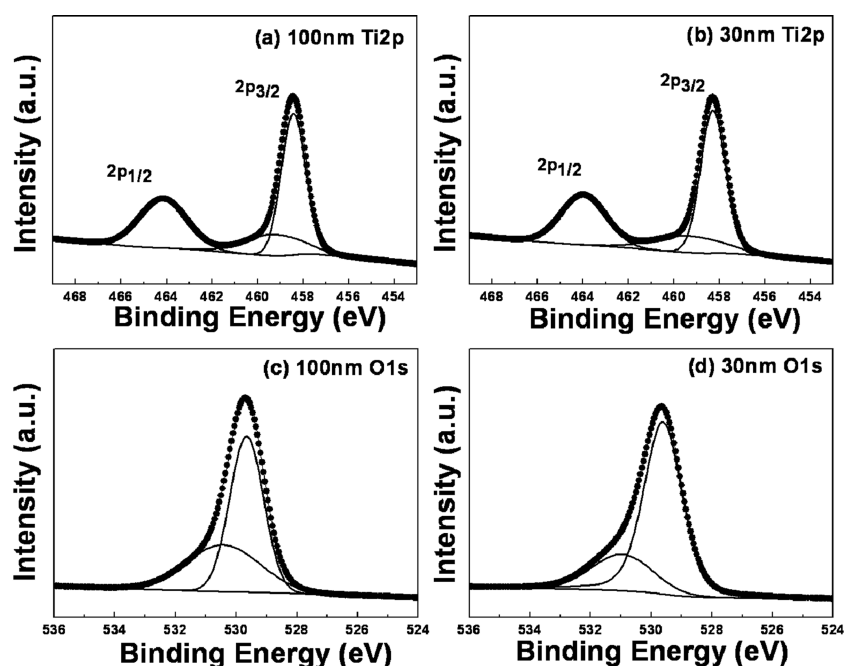


Fig. 4. The XPS core-level spectra for the Ti 2p_{1/2} and Ti 2p_{3/2} photoelectrons at ~458.4 eV and ~464.0 eV for the NWs fabricated with (a) ~100 nm and (b) ~30 nm in diameter, and the O 1s photoelectrons at ~530.9 eV for the samples fabricated with (c) ~100 nm and (d) ~30 nm in diameter.

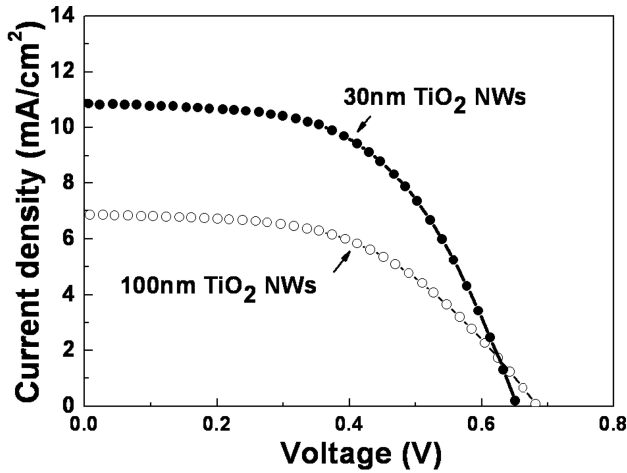


Fig. 6. Photocurrent-voltage curves obtained from the size-selected TiO₂ NWs fabricated with ~100 nm and ~30 nm in diameter.

via electrospinning, the major contribution is the bulk oxygen atoms on the TiO₂ NWs.

Figure 5 presents the UV-Vis absorption spectra relative to the light absorption properties for the size-selected TiO₂ NWs. The two types of size-selected TiO₂ NWs exhibit similar light absorption spectra. For the characteristic peak of the measured spectra, the band gap energy (E_g) of the TiO₂ NWs can be calculated by using the equation given below [19]:

$$E_g = h \cdot C / \lambda \quad (1)$$

Where h , C , and λ are the Planck constant ($= 6.626 \times 10^{-34}$ Joules·sec), the speed of light ($= 3.0 \times 10^8$ meter·sec⁻¹), and the characteristic wavelength, respectively. Two types of the size-selected TiO₂ NWs show characteristic peaks near ~380 nm equally. The results imply that the band gap energies of the two samples are ~3.2 eV ($1\text{eV} = 1.6 \times 10^{-19}$ Joules). This is in agreement with the well-known band gap energy of TiO₂. In other words, the band gap energy of electro-spun TiO₂ NWs with a ~30 nm diameter has the same value when compared to electro-spun TiO₂ NWs with a ~100 nm size.

Figure 6 shows photocurrent-voltage curves obtained from two types of electro-spun TiO₂ NWs with sizes of ~30 nm and ~100 nm in diameter. Short-circuit current densities (J_{sc}) for the two types of electro-spun TiO₂ NW photoelectrodes are 10.86 and 6.86 mA/cm², respectively. This implies that the short-circuit current density of a TiO₂ NW photoelectrode with a ~30 nm diameter improves by ~58% compared to that of a TiO₂ NW photoelectrode with a ~100 nm diameter because of the enhanced specific surface area available for a higher rate of dye adsorption resulting from a smaller size of the NW photoelectrode. The open-circuit voltage (V_{oc}) for all the samples is observed at 0.65–0.68 V. Two samples exhibit almost the same values because TiO₂ NW photoelectrodes are composed of

Table 1. Comparison of parameters of the dye-sensitized solar cells using electro-spun TiO₂ NWs with ~30 nm in diameter and a ~100 nm in diameter

Samples	J_{sc} (mA/cm ²)	V_{oc} (V)	ff (%)	η (%)
TiO ₂ -30 nm	10.86	0.65	55.19	3.93
TiO ₂ -100 nm	6.86	0.68	51.57	2.42

both the anatase phase and the rutile phase. In addition, a fill factor of TiO₂ NW photoelectrodes fabricated with a ~30 nm diameter (ff = 0.55) is slightly higher than that of TiO₂ NW photoelectrodes fabricated with a ~100 nm diameter (ff = 0.51). The overall efficiency (η) of all the samples was calculated from equation given below [3]:

$$\eta (\%) = [J_{sc} \times V_{oc} \times \text{ff}] / [I_{\text{max}} \times V_{\text{max}}] \quad (2)$$

Where J_{sc} and V_{oc} are the short-circuit current density and open-circuit voltage, ff is the fill factor, and I_{max} and V_{max} are the maximum power current and maximum power voltage, respectively. Therefore, the overall efficiencies (η) for the size-selected TiO₂ NW photoelectrodes with a ~100 nm diameter and a ~30 nm diameter improve from 2.42% to 3.93% as shown in Table 1, which indicates that there is an enhanced cell efficiency (~62%) of TiO₂ NW photoelectrodes. The improvement of cell efficiency is due to the increased specific surface area available for a higher rate of dye adsorption. Therefore, the electro-spun TiO₂ NWs fabricated with a ~30 nm diameter may be considered as a promising photoelectrode material for the fabrication of efficient DSSCs.

Conclusions

Two types of size-selected TiO₂ NW photoelectrodes, one with a ~30 nm diameter and one with ~100 nm diameter, were successfully fabricated via an electrospinning method and their size, structure, and optical properties were demonstrated by a variety of characterization techniques such as SEM, TEM, XRD, XPS, and UV-Visible spectrophotometer. TiO₂ NW photoelectrodes fabricated with a ~30 nm diameter exhibit superior short-circuit current density, fill factor, and cell efficiency compared to the TiO₂ NW photoelectrodes fabricated with a ~100 nm diameter due to an increased specific surface area available for a higher rate of dye adsorption.

Acknowledgement

This research was supported by Basic Science Research Program through the National Research Foundation of Korea (NRF) funded by the Ministry of Education, Science and Technology (2011-0005561) and Seoul National University of Science & Technology.

References

1. B. O'Regan and M. Gratzel, *Nature* 353 (1991) 737.
2. M. Gratzel, *Nature* 414 (2001) 338.
3. M. Gratzel, *J. Photochem. Photobiol. C* 4 (2003) 145.
4. C. Lao, Y. Chuai, L. Su, X. Liu, L. Huang, H. Cheng, and D. Zou, *Solar Energy Mater. Solar Cells* 85 (2005) 457.
5. Y. Zhang, L. Wu, E. Xie, H. Duan, W. Han, and J. Zhao, *J. Power Sources* 189 (2009) 1256.
6. H.-S. Shim, S.-I. Na, S.H. Nam, H.-J. Ahn, H.J. Kim, D.Y. Kim, and W.B. Kim, *Applied Physics Letters* 92 (2008) 183107.
7. K. Yu and J. Chen, *Nanoscale Res Lett.* 4 (2009) 1.
8. S. Barth, F. Hernandez-Ramirez, J.D. Holmes, and A. Romano-Rodriguez, *Progress in Materials Science* 55 (2010) 563.
9. K. Mukherjee, T.H. Teng, R. Jose, and S. Ramakrishna, *Appl. Phys. Lett.* 95 (2009) 012101.
10. K. Onozuka, B. Ding, Y. Tsuge, T. Naka, M. Yamazaki, S. Sugi, S. Ohno, M. Yoshikawa, and S. Shiratori, *Nanotechnology* 17 (2006) 1026.
11. J.K. Oh, J.K. Lee, H.S. Kim, S.B. Han, and K.W. Park, *Chem. Mater.* 22 (2010) 1114.
12. M. Law, L.E. Greene, J.C. Johnson, R. Saykally, and P.D. Yang, *Nat. Mater.* 4 (2005) 455.
13. S.Y. Jeong, H.Y. Ahn, T.Y. Seong, *Mater. Lett.* 65 (2011) 471.
14. J.B. Lee, S.Y. Jeong, W.J. Moon, T.Y. Seong, and H.Y. Ahn, *J. Alloys Compd.* 509 (2011) 4336.
15. S. Ramakrishna, K. Fujihara, W.E. Teo, T.C. Lim, and Z. Ma, *An Introduction to Electrospinning and Nanofibers*, World Scientific Publishing Co. Ltd., Singapore (2005) 7.
16. J.Y. Park, S.W. Choi, K. Asokan, and S.S. Kim, *Met. Mater. Int.* 16 (2010) 785.
17. J.F. Moulder, W.F. Stickle, P.E. Sobol, and K.D. Bomben, *Handbook of X-ray Photoelectron Spectroscopy*, Physical Electronics, Eden Prairie, MN, (1995).
18. H. Perron, J. Vandenborre, C. Domain, R. Drot, J. Roques, E. Simoni, J.-J. Ehrhardt, and H. Catalette, *Surf. Sci.* 601 (2007) 518.
19. Y. Haibin, Z. Jianhui, Y. Ruijin, and S. Qiang, *J. Rare Earth.* 27 (2009) 308.